Electronic Supplementary Information (ESI):

Self-template construction of hollow Co_3O_4 microspheres from porous ultrathin nanosheets and efficient noble-metal-free water oxidation catalysts

Jun Zhao,[a] Yong-Cun Zou,[a] Xiaoxin Zou,[a]* Tian-Yu Bai,[a] Yi-Pu Liu,[a] Rui-Qin Gao,[a] De-Jun Wang [a,b], and Guo-Dong Li[a]*

[a] State Key Laboratory of Inorganic Synthesis and Preparative Chemistry, College of Chemistry, Jilin University, Changchun 130012, P.R. China

[b] Department of Chemistry, Tsinghua University, Beijing 100084, P. R. China

* E-mail: G. D. Li, lgd@jlu.edu.cn;

X. X. Zou, chemistryzouxx@gmail.com

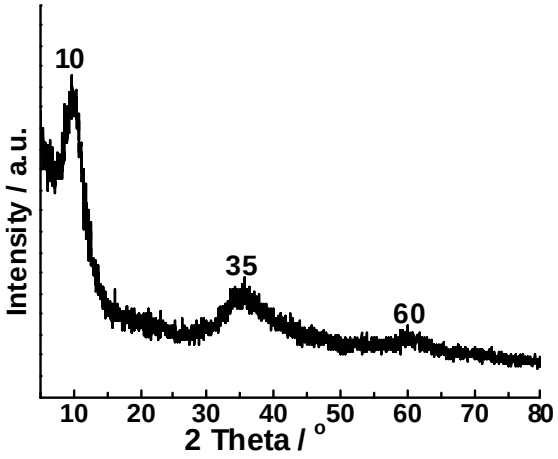

Fig. S1 XRD pattern of the *s*-CoA sample. The XRD pattern of the *s*-CoA sample showed diffraction peaks similar to those of previously-reported polyols-based metal alkoxides.[S1]

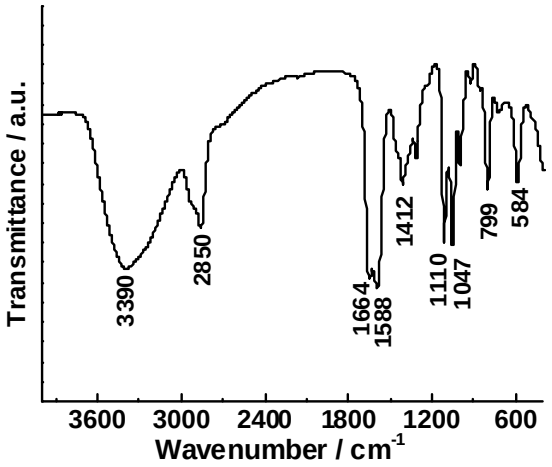

Fig. S2 IR spectrum of the *s*-CoA sample. The broad IR absorption band at ~3390 cm^{-1} is attributed to hydrogen-bound hydroxyl groups, and the absorption band at ~2850 cm^{-1} is characteristic of the C-H stretching vibrations. In addition, all the bands located below 2000 cm^{-1} are generally assigned to Co-O, C-C, C-C-O and C-O-Co groups. Similar IR results were also observed previously for other metal alkoxides.[S1-2]

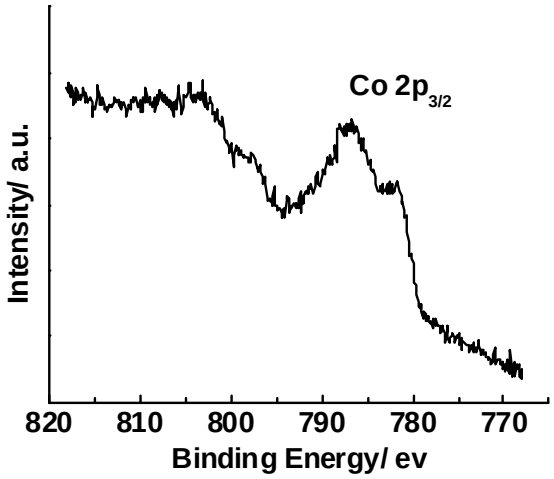

Fig. S3 Co 2p electron XPS spectrum for *s*-CoA spheres. Two $2P_{3/2}$ XPS peaks were detected at 786.6 and 802.8 eV, indicating the presense of Co (II) species.[S7]

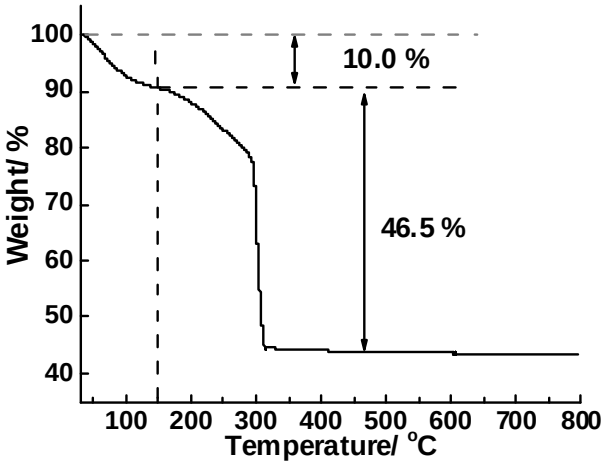

Fig. S4 TG curve measured in air for the *s*-CoA sample. TG analysis of *s*-CoA was carried out in air from 25 to 800 °C. Before 150 °C, the weight loss of 10.0% can be attributed to evaporation of the absorbed organic residues and water species on the *s*-CoA surface. The *s*-CoA completely decomposed at around 300 °C with a total weight loss of ~46.5 %. From the weight loss values it is estimated that the empirical composition of *s*-CoA is $C_3H_6O_3Co$.

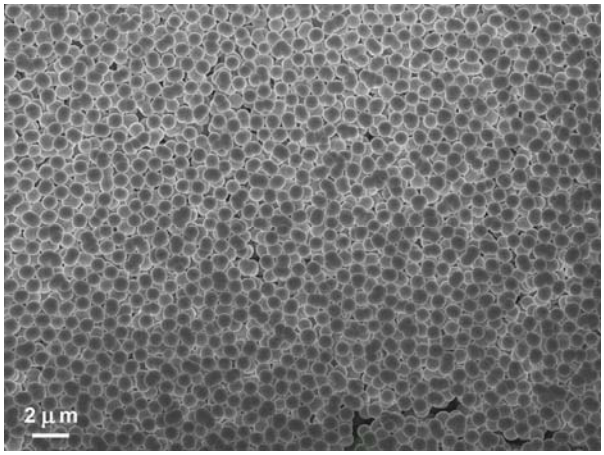

Fig. S5 SEM image of the composite of the *s*-CoA sample.

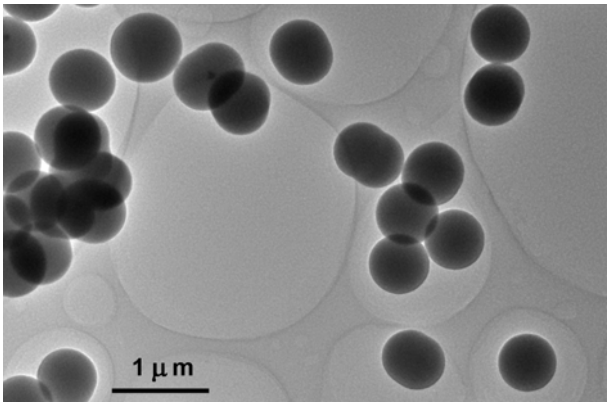

Fig. S6 TEM image of the *s*-CoA sample.

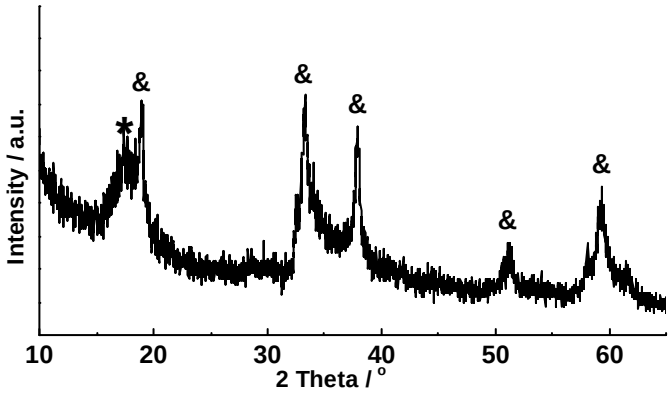

Fig. S7 XRD pattern of the *h*-CoOH sample. Fig. S7 reveals that *h*-CoOH possibly contains both *β*-$Co(OH)_2$ (which is marked by "&") and cobalt carbonate hydroxide ($Co(CO_3)_{0.5}(OH)\cdot 0.11H_2O$, which is marked by "*").

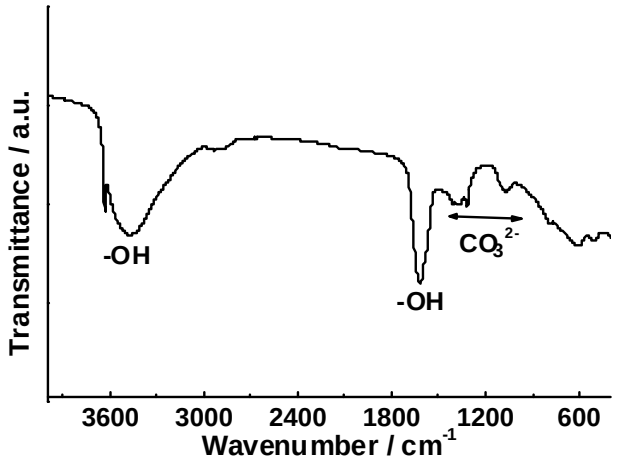

Fig. S8 IR spectrum of the *h*-CoOH sample. Comparison of the IR spectra of *s*-CoA and *h*-CoOH revealed that upon hydrothermal treatment the IR absorption bands for organic component in *s*-CoA (Fig. S2) disappeared, indicating the complete conversion of *s*-CoA into *h*-CoOH The broad IR absorption band at 2976-3680 cm^{-1} is due to stretching vibrations of -OH, and the absorption band at ~1620 cm^{-1} is due to bending vibration of -OH. This demonstrates that a large number of OH groups and water molecules exist in the *h*-CoOH sample. The weak absorption bands below 1500 cm^{-1} are attributed to the presence of a small amount if carbonate anions.[S3-5]

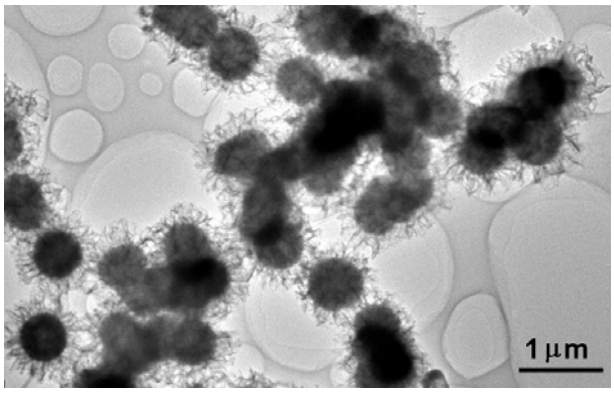

Fig. S9 TEM image of the product obtained after hydrothermal treatment of *s*-CoA for 15 min.

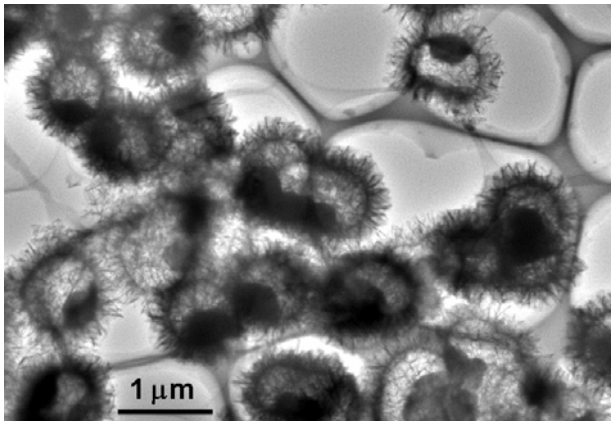

Fig. S10 TEM image of the product obtained after hydrothermal treatment of *s*-CoA for 60 min.

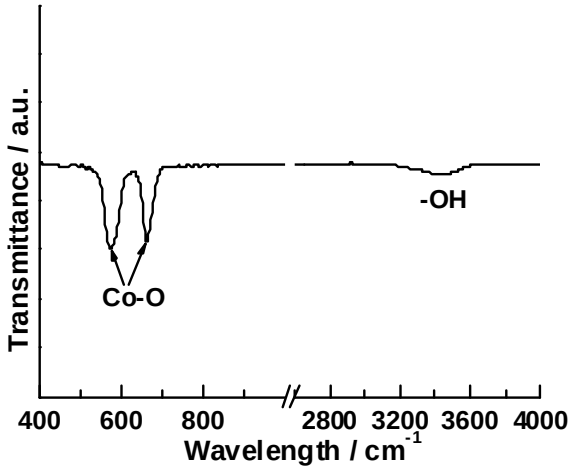

Fig. S11 IR spectrum of *h*-Co@200. The IR spectrum of *h*-Co@200 is in agreement with that of spinel Co_3O_4.[S6]

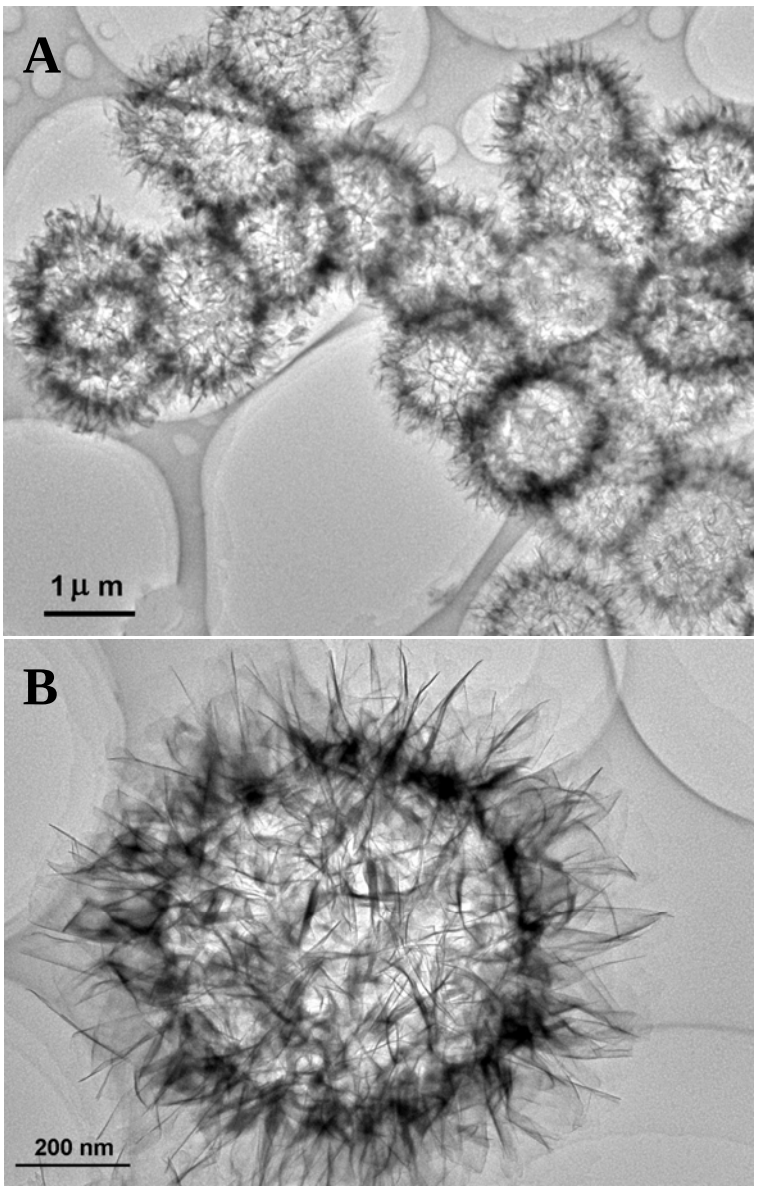

Fig. S12 TEM images of *h*-Co@200.

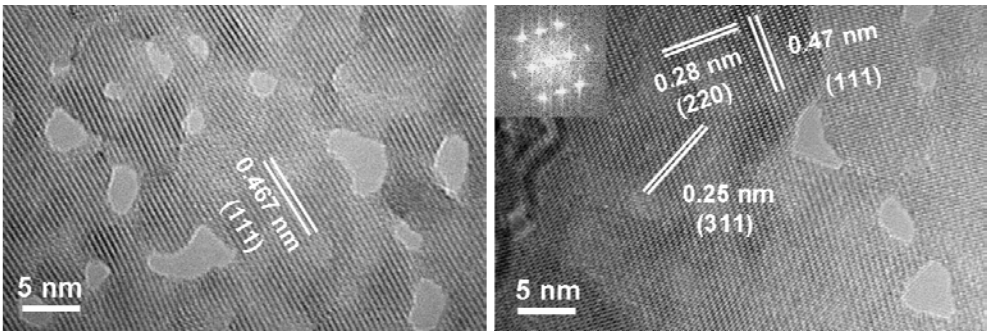

Fig. S13 HRTEM images of *h*-Co@200.

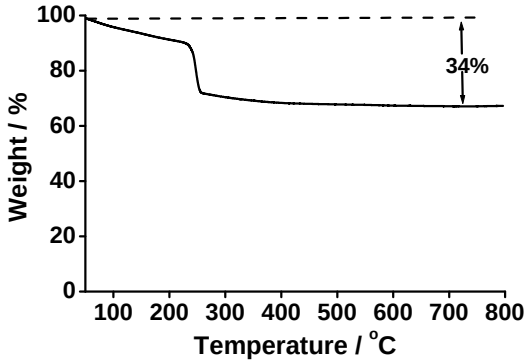

Fig. S14 Thermal gravimetric curve measured in air of *h*-CoOH. A total weight loss of about 34% is observed, and this weight loss is attributed to the removal of physically-adsorbed water molecules, and the release of H_2O and CO_2 of *h*-CoOH during the thermal treatment. The calculated weight losses from β-$Co(OH)_2$ to Co_3O_4 and from $Co(CO_3)_{0.5}(OH)\cdot 0.11H_2O$ to Co_3O_4 are about 14% and 24%, respectively. Because cobalt hydroxide has a strong ability to interact with water molecules, *h*-CoOH might adsorb a certain amount of H_2O on it. As a result, it is reasonable that a total weight loss of about 34% for *h*-CoOH was observed.

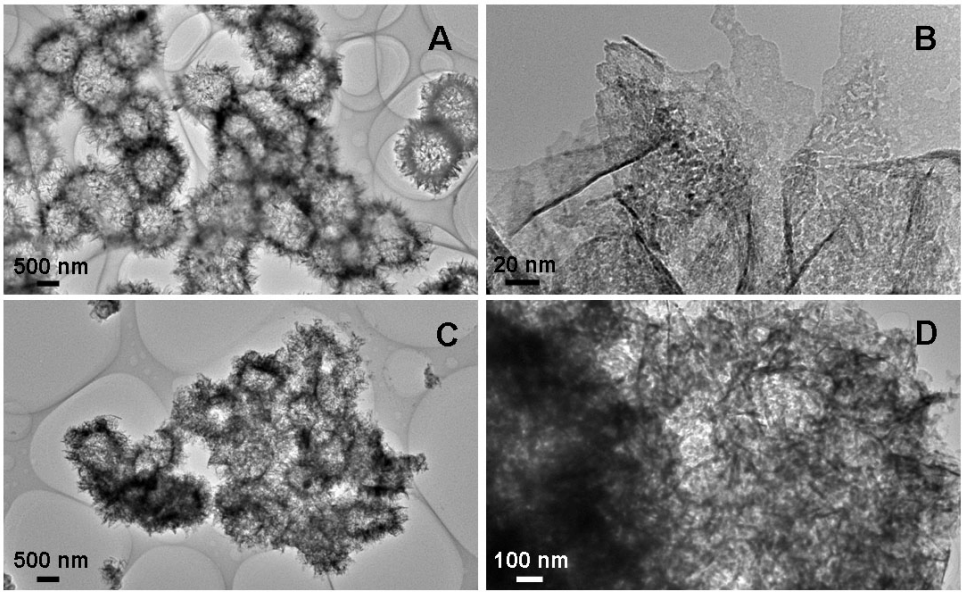

Fig. S15 HRTEM images of (A, B) *h*-Co@300 and (C, D) *h*-Co@400.

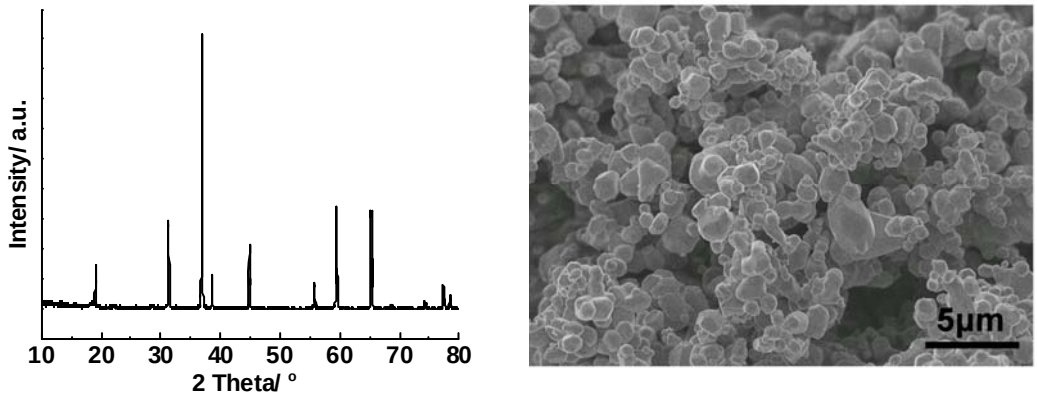

Fig. S16 XRD pattern (left) and SEM image (right) of Com-Co.

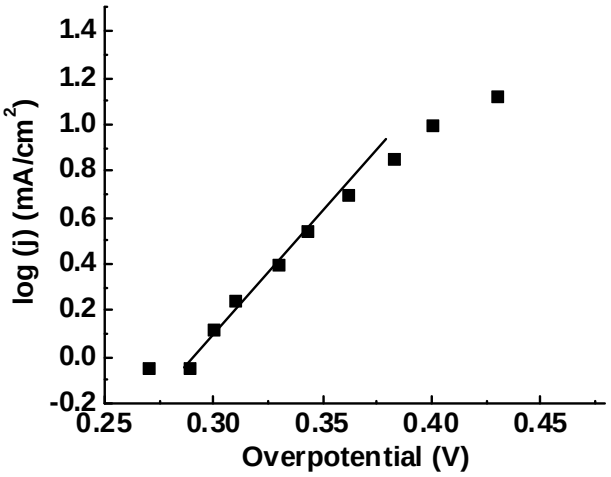

Fig. S17 Tafel plot for *h*-Co@200. To get the Tafel plot, we measured steady-state current as a function of voltage with a dwell time of 5 min.

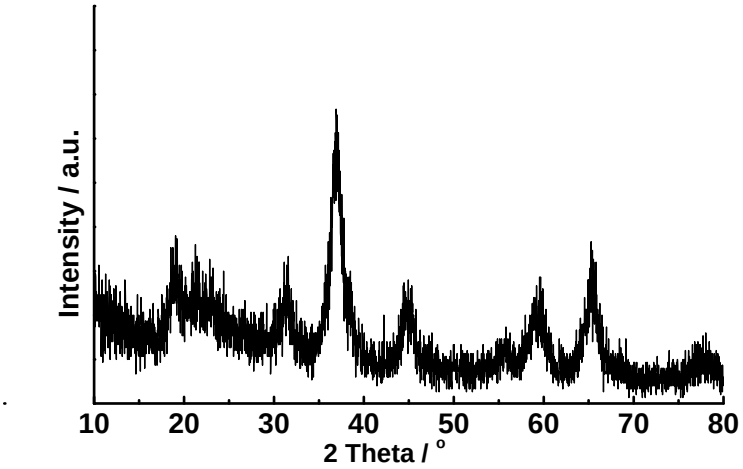

Fig. S18 XRD pattern of *h*-Co@200 after photocatalytic O_2 evolution reaction.

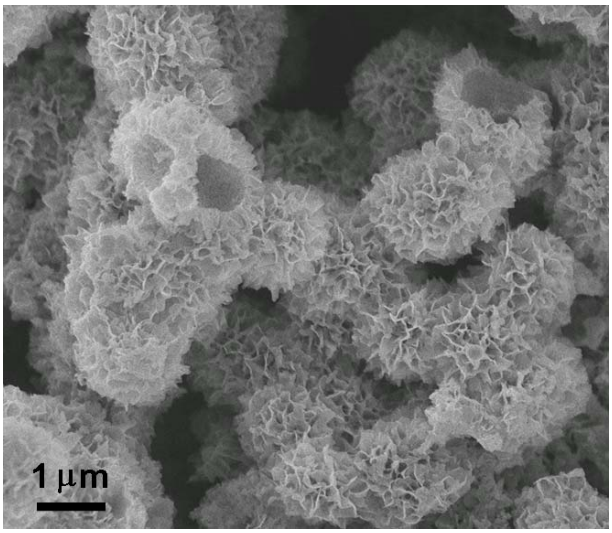

Fig. S19 SEM image of *h*-Co@200 after photocatalytic O_2 evolution reaction.

Table S1. TOFs of some recently-reported solid-state water oxidation electrocatalysts

Catalyst	TOF (S^{-1} Per Co/Mn atom)[a]	TOF (S^{-1} Per Co/Mn surface)[b]	Overpotential (mV)	pH	ref
Hollow Co_3O_4	**2.6×10^{-3}**	**0.20**	**400**	**13**	**This Work**
Co_3O_4 nanoparticle (< 5 nm)	—	0.21	314	14	*ACS Catal. 2013, **3**, 2497*
Co_3O_4 nanoparticle (~ 6 nm)	$1.87\times 10^{-2} \sim 9.3 \times 10^{-2}$	0.024-0.12	328	14	*J. Phys. Chem. C 2009, **113**, 15068*
Mesoporous Co_3O_4	$1.58 \times 10^{-3} \sim 4.55 \times 10^{-3}$	—	400	13	*Nano Research 2013, **6**, 47*
CoO_x film	3.2×10^{-3}	—	300	14	*J. Am. Chem. Soc. 2012, **134**, 17253*
Co-P film	7×10^{-4}	—	410	7.0	*Science 2008, **321**, 1072*
Zn-Co-LDH	6.1×10^{-2}	—	410	13	*J. Am. Chem. Soc. 2013,* 135, 17242-17245.
Co-Fe Prussion	2.6×10^{-3}	—	305	7.0	*J. Am. Chem. Soc. 2013, **135**, 13270*
Co-OEC	1.5×10^{-3}	—	400	7.0	*Energy Environ. Sci., 2011, **4**, 499*
MnO_x film	4×10^{-4}	—	300	14	*J. Am. Chem. Soc. 2012, **134**, 17253*

[a]TOF was calculated based on the assumption that all the Co ions present in the material were catalytically active. [b]TOF was calculated based on the assumption that all the surface Co ions present in the material were catalytically active.

Table S2. TOFs of some recently-reported solid-state water oxidation catalysts under visible light irradiation

Catalyst	TOF (S^{-1} Per Co/Mn atom)	ref
Hollow Co_3O_4	**2.7×10^{-4}**	**This Work**
Co_3O_4 supported in mesoporous silica	$2.12 \times 10^{-4} \sim 4.05 \times 10^{-4}$	*Angew. Chem. Int. Ed. 2009,**48**,1841* *ACS Catal. 2012, **2**, 2753*
Hierarchical porous Co_3O_4	2.4×10^{-4}	*J. Am. Chem. Soc. 2013, **135**, 4516*
Co_3O_4	1.4×10^{-4}	*J. Chem. Soc., Faraday Trans. 1, 1988, **84**, 2795*
$NiCo_2O_4$	7.9×10^{-5}	
$Li_2Co_2O_4$	1.0×10^{-3}	*Angew. Chem. Int. Ed. 2012, **51**, 1616*
$LaCoO_3$	6.5×10^{-4}	*Phys. Chem. Chem. Phys., 2012, **14**, 5753*
λ-MnO_2	$3 \times 10^{-5} \sim 5 \times 10^{-6}$	*J. Am. Chem. Soc. 2010, **132**, 11467*

ESI references:

[S1] D. Larcher, G. Sudant, R. Patrice, J.-M. Tarascon, *Chem. Mater.*, 2003, **15**, 3543.

[S2] J. Zhao, X.-X. Zou, J. Su, P.-P. Wang, L.-J. Zhou, G.-D. Li, *Dalton Trans.*, 2013, **42**, 4365.

[S3] J. Xiao, S. Yang, *J. Mater. Chem.*, 2012, **22**, 12253.

[S4] J. Li, H. Fan, X. Jia, *J. Phys. Chem. C*, 2010, **114**, 14684.

[S5] J. Zhang, S. Wang, M. Xu, Y. Wang, B. Zhu, S. Zhang, W. Huang, S. Wu, *Cryst. Growth Des.*, 2009, **9**, 3532.

[S6] X. Zou, J. Su, R. Silva, A. Goswami, B. R. Sathe, T. Asefa, *Chem. Commun.*, 2013, **49**, 7522.

[S7] R. Shi, G. Chen, W. Ma, D. Zhang, G. Qiua, X. Liu, *Dalton Trans.*, 2012, **41**, 5981.